FERMILAB-CONF-05-226-E

TOP QUARK PRODUCTION AND PROPERTIES AT THE TEVATRON

Frank Fiedler
Munich University (LMU), Germany
on behalf of the CDF and DØ Collaborations

Abstract

The precise measurement of top quark production and properties is one of the primary goals of the Tevatron during Run II. The total $t\bar{t}$ production cross-section has been measured in a large variety of decay channels and using different selection criteria. Results from differential cross-section measurements and searches for new physics in $t\bar{t}$ production and top quark decays are available. Electroweak production of single top quarks has been searched for. The results from all these analyses, using typically $200\,\mathrm{pb}^{-1}$ of data, are presented.

1 Introduction

The top quark is special among the fermions of the Standard Model because of its large mass. Currently, the top quark can only be studied at the two Tevatron experiments CDF and DØ, where measurements of top quark production and properties are one of the key physics goals of Run II.

The top quark mass is discussed in a separate article [1]. This article focuses on measurements of the total $t\bar{t}$ production cross-section, searches for new physics in $t\bar{t}$ production and top quark decay, and on the search for electroweak (single) top quark production. While the CDF and DØ experiments have both collected more than $500\,\mathrm{pb}^{-1}$ of data so far during Tevatron Run II, surpassing the Run I integrated luminosity by a factor ≥ 5, the measurements summarized in this article typically use about $200\,\mathrm{pb}^{-1}$.

In section 2, general aspects of top production and event topologies at the Tevatron are briefly discussed. Section 3 discusses the measurements of the total $t\bar{t}$ production cross-section, while further measurements in $t\bar{t}$ events are presented in section 4. The search for single top quark production is presented in section 5.

2 Top Quark Production at the Tevatron

In the Standard Model, the production of top quarks at a hadron collider can in principle proceed via two mechanisms: $t\bar{t}$ pair production via the strong interaction, and single top (or antitop) production via the electroweak interaction. The leading order Feynman diagrams are shown in figure 1 together with the Standard Model cross-sections in $p\bar{p}$ collisions at a centre-of-mass energy of 1.96 TeV (corresponding to the Tevatron collider at Run II) [2, 3].

In the following, the main characteristics of $t\bar{t}$ and single top events at the Tevatron are discussed.

2.1 Classification of $t\bar{t}$ Event Topologies

In the Standard Model, the branching fraction of top quark decays to a b quark and an on-shell W boson is close to 100%, other decay modes not being observable with Tevatron luminosities. The subsequent W decays determine the event topology seen in the detector, and $t\bar{t}$ events are classified as follows:

- **Dilepton events**, where both W bosons decay into an $e\nu$ or $\mu\nu$ final state, are characterized by two energetic, isolated leptons of opposite charge, two energetic b jets, and missing transverse energy. While the product branching ratio is only about 5%, pure event samples can be obtained requiring the two leptons in the event to be reconstructed.

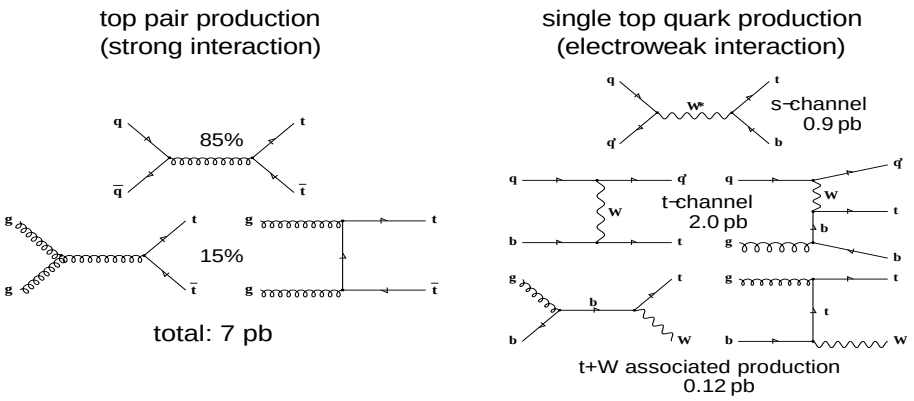

Figure 1: *Leading order Feynman diagrams for top quark production at hadron colliders together with the Standard Model cross-sections at the Tevatron.*

- In **lepton+jets events**, one W boson decays hadronically and the other into an $e\nu$ or $\mu\nu$ final state. This topology is characterized by an energetic, isolated electron or muon, four energetic jets (two b jets and two light-quark jets from the W decay), and missing transverse energy. The product branching ratio of $\approx 30\%$ is larger than for dilepton events, and the main background is from W+jets events.
- In **hadronic events**, one expects 6 energetic jets (of which two are b jets) and no significant missing transverse energy. Because of large backgrounds from QCD jet production, identifying $t\bar{t}$ events in the hadronic channel is challenging, despite the large product branching ratio of $\approx 44\%$.
- In about 21% of the $t\bar{t}$ events, at least one W boson decays into a $\boldsymbol{\tau\nu}$ **final state**. Depending on its decay, the τ lepton can be identified as a narrow jet, an isolated track, or an electron or muon. Two energetic b jets, missing transverse energy, and the decay products from the second W boson complete the event topology.

In general, the reconstruction and selection of $t\bar{t}$ event candidates is based on reconstructing the directions and energies/momenta of isolated electrons or muons and jets, and on reconstructing the missing transverse energy $\not\!\!E_T$ from the transverse momentum balance in the event. The purity of the event samples can be enhanced by identifying jets that originated from a b quark (b tagging), since in the Standard Model, every $t\bar{t}$ event contains two b jets. Both CDF and DØ use

- secondary vertex algorithms, based on explicit reconstruction of the decay vertex of the b hadron within the jet;
- impact parameter based algorithms that classify tracks inside a jet ac-

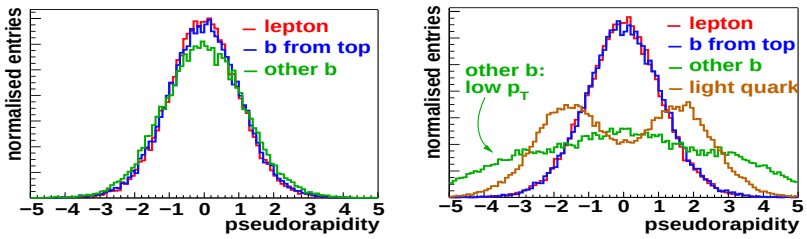

Figure 2: *Expected pseudorapidity distributions of the charged lepton and jets in single top events (left: s-channel, right: t-channel)* [4].

cording to their distance of closest approach to the primary event vertex; and

- soft leptons from semileptonic bottom or charm hadron decay (only muons are used so far)

to identify b jets. The requirements on the jet multiplicity, the minimum jet transverse energies, b identification of the jets, and event kinematic information can be balanced to minimize the measurement error; depending on the selection, not all jets need to be explicitly reconstructed.

2.2 Single Top Quark Production

The total cross-section for single top quark production is only a factor ~2 smaller than that for $t\bar{t}$ production; however, the relevant backgrounds are substantially larger (W+2jet instead of W+4jet events). To reduce the background, the selection of single top event candidates focuses on top decays with leptonic W decays and on the identification of the b jet(s) in the event. Figure 2 shows the expected pseudorapidity distributions of the charged lepton and jets in single top events. For s-channel events, two b jets are expected in the center of the detector. In general only one b jet can be reconstructed in case of the t-channel, but here an additional light quark jet can be observed.

3 Measurements of the Total $t\bar{t}$ Production Cross-Section

The goal is to measure the $t\bar{t}$ cross-section in as many different modes as possible to check the predictions of the Standard Model. The measurements in the different channels are described in the following sub-sections.

3.1 Lepton+Jets Channel, Topological Analyses

Both CDF and DØ have measured the $t\bar{t}$ cross-section in the lepton+jets channel without relying on b jet identification. In the CDF analysis [5], events with

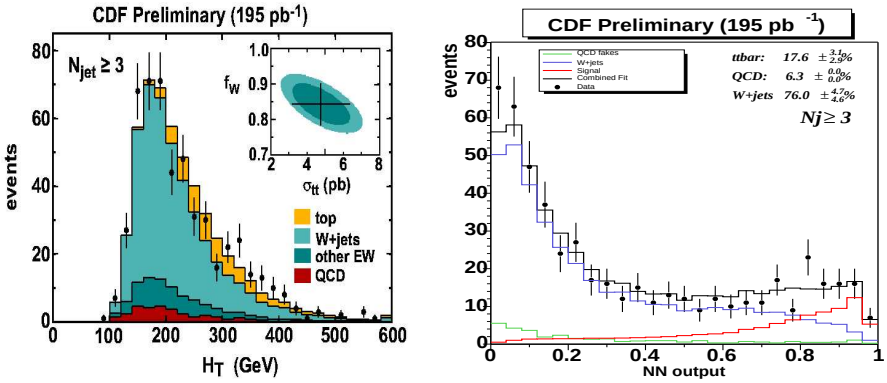

Figure 3: *CDF $t\bar{t}$ cross-section measurement in the lepton+jets channel using topological information. Left: H_T distribution. Right: NN output.*

one isolated electron with $E_T > 20\,\mathrm{GeV}$ or muon with $p_T > 20\,\mathrm{GeV}$, missing transverse energy $\not\!\!E_T > 20\,\mathrm{GeV}$, and at least 3 jets with $E_T > 15\,\mathrm{GeV}$ within the pseudorapidity range $|\eta| < 2.0$ are selected. For $\not\!\!E_T < 30\,\mathrm{GeV}$, there is an additional cut requiring the angle $\Delta\phi$ between the missing transverse energy and the highest E_T jet in the transverse plane to satisfy $0.5 < \Delta\phi < 2.5$. After this selection, the $t\bar{t}$ signal can be seen in the H_T distribution (H_T is the scalar sum of transverse energies of the lepton, jets, and the missing transverse energy) as shown in figure 3, and the $t\bar{t}$ cross-section is measured to be

$$\sigma(t\bar{t}) = (4.7 \pm 1.6(\mathrm{stat.}) \pm 1.8(\mathrm{syst.}))\ \mathrm{pb} \tag{1}$$

using a $195\,\mathrm{pb}^{-1}$ data sample. To optimise the measurement, 7 quantities have been chosen for training a neural network (NN) to separate the $t\bar{t}$ signal from the background. The NN output distribution is also shown in figure 3. From a fit to this distribution a result of

$$\sigma(t\bar{t}) = (6.7 \pm 1.1(\mathrm{stat.}) \pm 1.6(\mathrm{syst.}))\ \mathrm{pb} \tag{2}$$

is obtained from the same dataset. In both analyses, the main systematic error is from the uncertainty in the jet energy scale; it is however reduced from 30% in the H_T based measurement to 16% in the optimised analysis.

In the DØ topological analysis [6], events with one isolated electron or muon with $p_T > 20\,\mathrm{GeV}$, missing transverse energy ($\not\!\!E_T > 20$ GeV in the e+jets case and $\not\!\!E_T > 17\,\mathrm{GeV}$ for μ+jets events), and at least four jets with $E_T > 15\,\mathrm{GeV}$ within $|\eta| < 2.5$ are selected. So in contrast to CDF, four jets are required to be reconstructed, but a larger pseudorapidity region is allowed. To

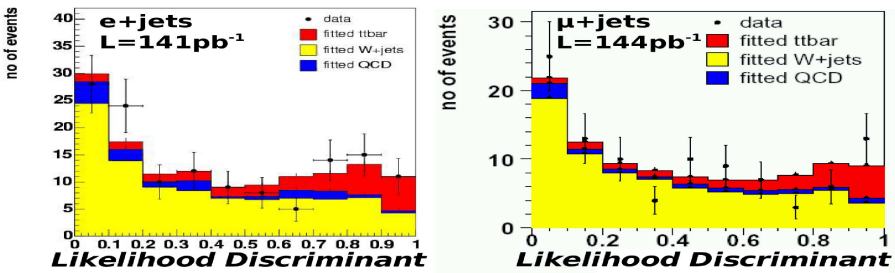

Figure 4: *DØ $t\bar{t}$ cross-section measurement in the lepton+jets channel using topological information. The likelihood discriminant distributions are shown for e+jets (left) and μ+jets (right) events together with the fitted $t\bar{t}$ and background contributions.*

further separate $t\bar{t}$ events from background, a likelihood is constructed using angular variables and ratios of energy dependent variables, to avoid direct dependence on the jet energy scale. The resulting distributions are given in figure 4. The combined fit to the e+jets and μ+jets distributions from $141 - 144\,\mathrm{pb}^{-1}$ of data yields

$$\sigma(t\bar{t}) = \left(7.2^{+2.6}_{-2.4}(\mathrm{stat.})^{+1.6}_{-1.7}(\mathrm{syst.}) \pm 0.5(\mathrm{lumi.})\right)\ \mathrm{pb}\ . \tag{3}$$

3.2 Lepton+Jets Channel, b Tagging Analyses

For the DØ measurements that make use of lifetime b tagging information [7], events are selected with the same criteria as above. The $t\bar{t}$ cross-section is then determined from a combined fit to the jet multiplicity distributions for events with exactly one b tagged jet and events with at least two b tagged jets. Using a data sample of $158 - 169\,\mathrm{pb}^{-1}$, DØ obtains

$$\sigma(t\bar{t}) = \left(8.2 \pm 1.3(\mathrm{stat.})^{+1.9}_{-1.6}(\mathrm{syst.}) \pm 0.5(\mathrm{lumi.})\right)\ \mathrm{pb} \tag{4}$$

using secondary vertex b tagging and

$$\sigma(t\bar{t}) = \left(7.2^{+1.3}_{-1.2}(\mathrm{stat.})^{+1.9}_{-1.4}(\mathrm{syst.}) \pm 0.5(\mathrm{lumi.})\right)\ \mathrm{pb} \tag{5}$$

with a track impact parameter based algorithm. The jet multiplicity distributions obtained with secondary vertex b tagging are shown in figure 5. In a separate analysis, DØ analyzes events with a semimuonic bottom or charm decay, resulting in [8]

$$\sigma(t\bar{t}) = (11.2 \pm 4.0(\mathrm{stat.}) \pm 1.3(\mathrm{syst.}) \pm 1.1(\mathrm{lumi.}))\ \mathrm{pb} \tag{6}$$

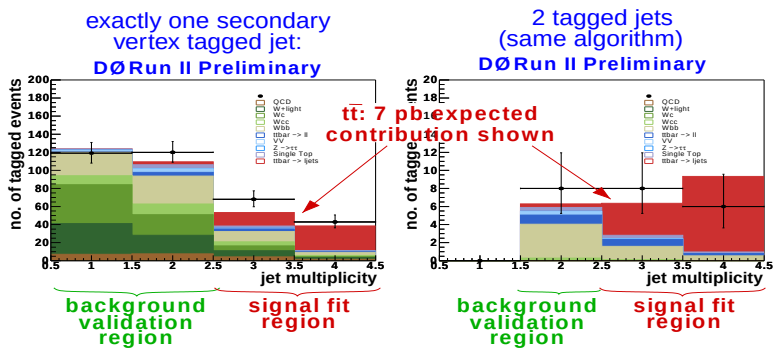

Figure 5: *DØ $t\bar{t}$ cross-section measurement in the lepton+jets channel using b tagging information. The jet multiplicity distributions for single and double secondary vertex tagged events are shown together with the expected Standard Model signal and background.*

based on $93\,\mathrm{pb}^{-1}$.

Several CDF analyses make use of b tagging information. The preselection of events requires one lepton, missing transverse energy, and three jets as in section 3.1. When at least one jet is required to be secondary vertex tagged [9], a measurement of

$$\sigma(t\bar{t}) = \left(5.6^{+1.2}_{-1.1}(\mathrm{stat.})^{+0.9}_{-0.6}(\mathrm{syst.})\right)\ \mathrm{pb} \tag{7}$$

is obtained from the jet multiplicity distribution (where a value of $H_T > 200\,\mathrm{GeV}$ is required for events with three or more jets) in $162\,\mathrm{pb}^{-1}$ shown in figure 6. Alternatively, the fraction of $t\bar{t}$ events in events with at least 3 jets is obtained from a fit to the E_T distribution of the leading jet, which is also shown in figure 6, yielding [10]

$$\sigma(t\bar{t}) = (6.0 \pm 1.6(\mathrm{stat.}) \pm 1.2(\mathrm{syst.}))\ \mathrm{pb}\ . \tag{8}$$

For the CDF multiple tag analysis, a special version of the b tagging algorithm has been developed with looser criteria to increase the statistics. From the jet multiplicity distributions obtained with the regular and the loose b tag, measurements of [9, 11]

$$\sigma(t\bar{t}) = \left(5.0^{+2.4}_{-1.9}(\mathrm{stat.})^{+1.1}_{-0.8}(\mathrm{syst.})\right)\ \mathrm{pb} \qquad \text{(regular b tag) and} \tag{9}$$

$$\sigma(t\bar{t}) = \left(8.2^{+2.4}_{-2.1}(\mathrm{stat.})^{+1.8}_{-1.0}(\mathrm{syst.})\right)\ \mathrm{pb} \qquad \text{(loose b tag)} \tag{10}$$

are obtained. Finally, CDF also uses events with b jets identified by an impact parameter based algorithm, yielding [12]

$$\sigma(t\bar{t}) = \left(5.8^{+1.3}_{-1.2}(\mathrm{stat.}) \pm 1.3(\mathrm{syst.})\right)\ \mathrm{pb} \tag{11}$$

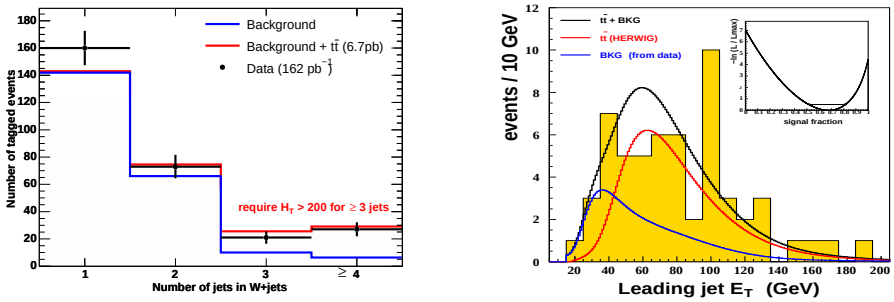

Figure 6: *CDF $t\bar{t}$ cross-section measurement in the lepton+jets channel using b tagging information. Left: the jet multiplicity distribution for events with at least one b tagged jet. Right: the leading jet E_T distribution for events with at least 3 jets.*

in $162\,\mathrm{pb}^{-1}$, as well as events with a semimuonic bottom or charm hadron decay, resulting in [13]

$$\sigma(t\bar{t}) = \left(5.2^{+2.9}_{-1.9}(\mathrm{stat.})^{+1.3}_{-1.0}(\mathrm{syst.})\right)\ \mathrm{pb} \tag{12}$$

using $200\,\mathrm{pb}^{-1}$.

3.3 Dilepton Channel

The CDF selection of $t\bar{t}$ events in the dilepton channel requires two isolated tracks ($p_T > 20\,\mathrm{GeV}$) and missing transverse energy ($\not\!\!E_T > 25\,\mathrm{GeV}$). The $t\bar{t}$ production cross-section is determined from the jet multiplicity distribution of events where both tracks are identified as leptons, or events where only one identified lepton is required. The combined result is [14]

$$\sigma(t\bar{t}) = \left(7.0^{+2.4}_{-2.1}(\mathrm{stat.})^{+1.6}_{-1.1}(\mathrm{syst.}) \pm 0.4(\mathrm{lumi.})\right)\ \mathrm{pb} \tag{13}$$

using $200\,\mathrm{pb}^{-1}$. The jet multiplicity distribution for the analysis with at least one identified lepton is shown in figure 7. One of the main backgrounds to $t\bar{t}$ production in the dilepton channel is diboson (mostly WW) production. In a separate analysis, CDF fits the two-dimensional jet multiplicity vs. $\not\!\!E_T$ distribution to measure the $t\bar{t}$, WW, and $Z \to \tau\tau$ cross-sections simultaneously. This analysis yields [15]

$$\sigma(t\bar{t}) = \left(8.6^{+2.5}_{-2.4}(\mathrm{stat.}) \pm 1.1(\mathrm{syst.})\right)\ \mathrm{pb} \tag{14}$$

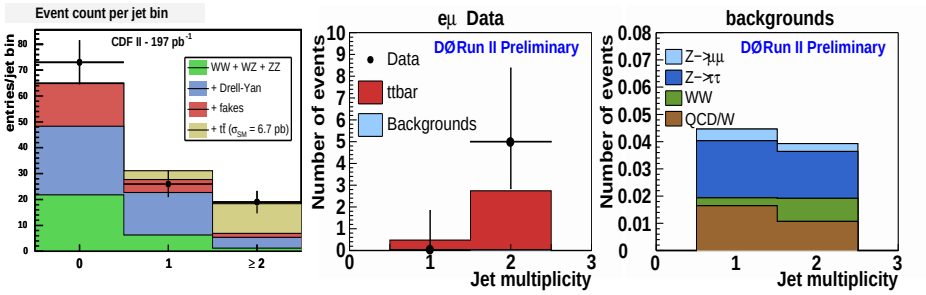

Figure 7: *CDF and DØ $t\bar{t}$ cross-section measurements in the dilepton channel. Left: jet multiplicity distribution in the CDF "lepton+track" analysis. Middle and right: jet multiplicity distributions for data (middle) and expected background (right) in the DØ dilepton measurement with at least one secondary vertex b tagged jet.*

For the DØ dilepton analysis, events with two isolated leptons with $p_T > 15\,\mathrm{GeV}$ ($p_T > 20\,\mathrm{GeV}$ in the dielectron channel), two jets with $E_T > 20\,\mathrm{GeV}$, missing transverse energy $\not\!\!E_T > 35\,\mathrm{GeV}$ ($\not\!\!E_T > 25\,\mathrm{GeV}$ in the $e\mu$ channel), and $H_T^{\mathrm{lead.}\ \ell} > 120(140)\,\mathrm{GeV}$ in the $\mu\mu$ ($e\mu$) channel are selected, where $H_T^{\mathrm{lead.}\ \ell}$ includes all jets and the leading lepton. Additional cuts reject events consistent with a $Z \to \ell\ell$ hypothesis. With no b tagging criteria applied, the analysis yields [16]

$$\sigma(t\bar{t}) = \left(14.3^{+5.1}_{-4.3}(\mathrm{stat.})^{+2.6}_{-1.9}(\mathrm{syst.}) \pm 0.9(\mathrm{lumi.})\right)\ \mathrm{pb} \tag{15}$$

using $140 - 156\,\mathrm{pb}^{-1}$. When requiring at least one jet to be secondary vertex b tagged, the $e\mu$ channel alone yields [17]

$$\sigma(t\bar{t}) = \left(11.1^{+5.8}_{-4.3}(\mathrm{stat.}) \pm 1.4(\mathrm{syst.}) \pm 0.7(\mathrm{lumi.})\right)\ \mathrm{pb} \tag{16}$$

with a very high purity sample, see figure 7.

3.4 Hadronic Channel

To separate $t\bar{t}$ events in the hadronic channel from the large multijet background, both tight kinematic cuts and b tagging information are applied. CDF selects events with 6 to 8 jets and no isolated leptons and applies kinematic cuts. In the distribution of the number of b tagged jets as a function of jet multiplicity (see figure 8) the $t\bar{t}$ cross-section is then measured to be [18]

$$\sigma(t\bar{t}) = \left(7.8 \pm 2.5(\mathrm{stat.})^{+4.7}_{-2.3}(\mathrm{syst.})\right)\ \mathrm{pb} \tag{17}$$

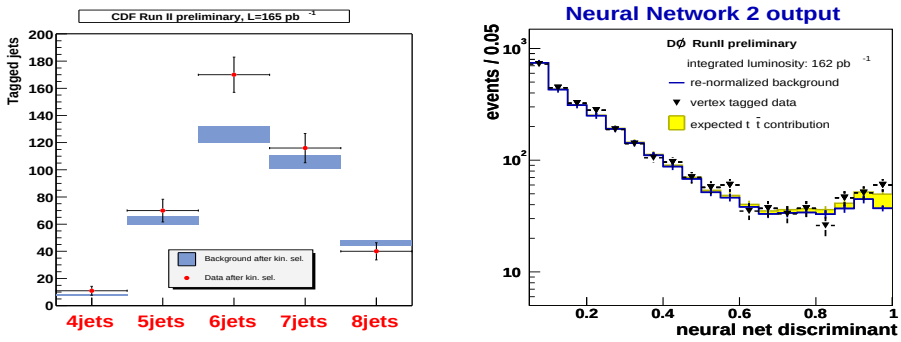

Figure 8: *CDF and DØ $t\bar{t}$ cross-section measurements in the hadronic channel. Left: number of b tagged jets in the CDF event sample as a function of jet multiplicity. Right: output of the final NN in the DØ analysis.*

in $165\,\mathrm{pb}^{-1}$.

DØ selects events with 6 or more jets, of which exactly one is required to be b tagged. A chain of NNs feeding into each other is used, and the $t\bar{t}$ cross-section is determined from the excess of events after a cut on the last NN output over background. A data sample of $162\,\mathrm{pb}^{-1}$ yields [19]

$$\sigma(t\bar{t}) = \left(7.7^{+3.4}_{-3.3}(\mathrm{stat.})^{+4.7}_{-3.8}(\mathrm{syst.}) \pm 0.5(\mathrm{lumi.})\right)\ \mathrm{pb}\ . \tag{18}$$

3.5 Events with $W \to \tau\nu$ Decays

CDF searches for $t\bar{t}$ events where one W decays electronically or muonically, while the other decays into a $\tau\nu$ final state with a subsequent τ decay into hadron(s) and a neutrino [20]. Events with an electron or muon with $E_T > 20\,\mathrm{GeV}$, a tau lepton with $E > 15\,\mathrm{GeV}$ and opposite charge, missing transverse energy $\not\!\!E_T > 20\,\mathrm{GeV}$, at least two jets ($E_T(1) > 25\,\mathrm{GeV}$, $E_T(2) > 15\,\mathrm{GeV}$), and $H_T > 205\,\mathrm{GeV}$ are selected. The two events observed in $193.5\,\mathrm{pb}^{-1}$ are consistent with the Standard Model expectation, and a limit of

$$Br(t \to b\tau\nu) < 5.0 \cdot Br_{\mathrm{SM}}(t \to b\tau\nu) \tag{19}$$

is derived at 95% confidence level.

3.6 Summary of $t\bar{t}$ Cross-Section Measurements

The $t\bar{t}$ cross-section measurements at Tevatron Run II are summarized in figure 9. The measurements in all decay channels and by both CDF and DØ are

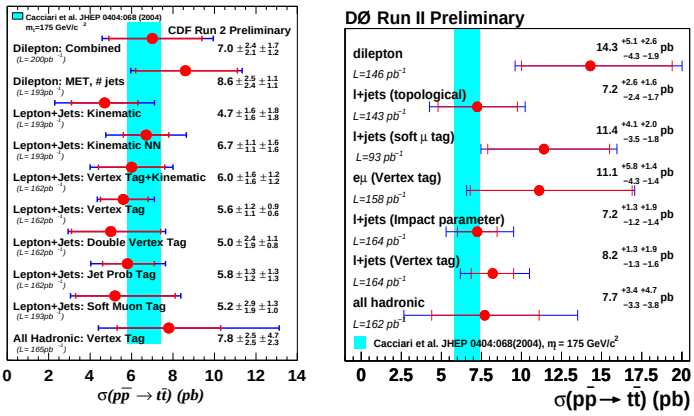

Figure 9: *A summary of all Tevatron Run II $t\bar{t}$ cross-section measurements by CDF (left) and DØ (right).*

mutually consistent and consistent with the prediction of the Standard Model.

4 Further $t\bar{t}$ Measurements

It is conceivable that physics beyond the Standard Model does not change the total $t\bar{t}$ cross-section, but either only affects differential cross-sections or top quark decays.

4.1 Searches for New Physics in $t\bar{t}$ Production

In a model independent analysis, CDF have searched for anomalous kinematic properties in their dilepton $t\bar{t}$ sample [21]. Four kinematic distributions where new physics signatures are expected to be likely to be seen were chosen a priori. While one of them, the leading lepton p_T spectrum shown in figure 10, shows an excess at low transverse momenta in 193 pb^{-1}, the other distributions agree with the expectation. The overall compatibility with the Standard Model prediction has been computed to be in the $1.0 - 4.5\%$ range.

CDF searches explicitly for production of fourth generation quarks [22]. If these t' quarks are heavier than the top quark, an excess of events at large H_T is expected. From a fit to the measured H_T distribution, which is consistent with the Standard Model expectation, upper limits on the cross-section of $t'\overline{t'}$ events can be placed, see figure 11.

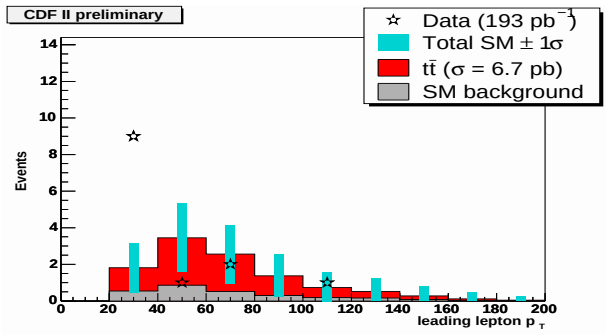

Figure 10: *CDF search for anomalous dilepton event properties. The p_T spectrum of the leading charged lepton in dilepton $t\bar{t}$ events at CDF.*

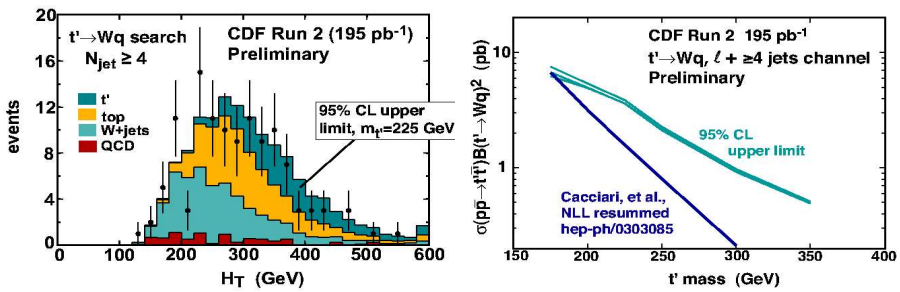

Figure 11: *CDF t' search. The H_T distribution in W+4jets events at CDF with a topological selection is shown with a fit that includes a component from hypothetical t' quark production (left). The resulting t' cross-section limits as a function of assumed t' mass are also shown (right).*

4.2 Searches for New Physics in Top Quark Decays

The Standard Model predicts the fractions of longitudinal and left-handed W bosons from top decay to be $F_0 = 1/(1 + 2m_W^2/m_{top}^2) \approx 0.7$ and $F_- = 1 - F_0$, while the fraction F_+ of right-handed W bosons is essentially zero because the bottom quarks from top quark decay are left-handed due to the large mass difference between top and bottom quarks. The predicted distribution of the decay angle θ^* in the W rest frame is shown in figure 12. From measurements of this distribution (or quantities that depend on $\cos\theta^*$), one can either search for non-zero constributions from right-handed W bosons ($F_+ > 0$) or, assuming $F_+ = 0$, for deviations from the predicted ratio F_0/F_-.

CDF have measured the fraction F_0 from the charged lepton p_T spectrum

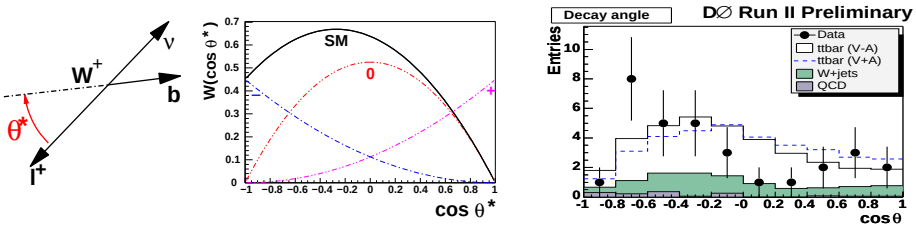

Figure 12: *W helicity measurements. The definition of the angle θ^* in the W rest frame (left) and the expected $\cos\theta^*$ distribution (middle), compared with the measured $\cos\theta^*$ distribution in b tagged lepton+jets events from $159-169\,\mathrm{pb}^{-1}$ at DØ (right).*

(using $200\,\mathrm{pb}^{-1}$) to be [23]

$$F_0 = 0.27^{+0.35}_{-0.24}\ , \tag{20}$$

and from explicit reconstruction of the value of $\cos\theta^*$ (using $162\,\mathrm{pb}^{-1}$) [24] to be

$$F_0 = 0.89^{+0.30}_{-0.34}(\mathrm{stat.}) \pm 0.17(\mathrm{syst.})\ , \tag{21}$$

respectively – to be compared with the DØ Run I value of [25] $F_0 = 0.56 \pm 0.31$. All of these values are consistent with the Standard Model expectation.

The two DØ measurements both use explicit $\cos\theta^*$ reconstruction in an event sample obtained with a topological [26] selection or using b tagging [27] in $159-169\,\mathrm{pb}^{-1}$. The $\cos\theta^*$ distribution from the b tagging analysis is shown in figure 12. Both analyses each yield a limit of

$$F_+ < 0.24 \text{ at } 90\% \text{ confidence level}, \tag{22}$$

to be compared with the CDF Run I exclusion limit of $F_+ < 0.18$ at 95% confidence level [28].

In supersymmetric models with $m_{H^\pm} < m_{top}$, the top quark may decay into a charged Higgs and a bottom quark. Depending on the values of $\tan\beta$ and $m_{H^\pm}$, one expects the following changes in the observed $t\bar{t}$ event topologies [29]:

- an excess of τ decays due to $H^+ \to \tau^+\nu$ decays for large $\tan\beta$,
- an excess of hadronic top decays due to $H^+ \to c\bar{s}$ decays for small $\tan\beta$ and small $m_{H^\pm}$, or
- $t\bar{t}$ events with two extra b jets from $H^+ \to W^+b\bar{b}$ decays for small $\tan\beta$ and large $m_{H^\pm}$.

The CDF collaboration has therefore taken their measurements of the $t\bar{t}$ cross-section in the dilepton and lepton+jets channels as well as their limit on $t\bar{t} \to$

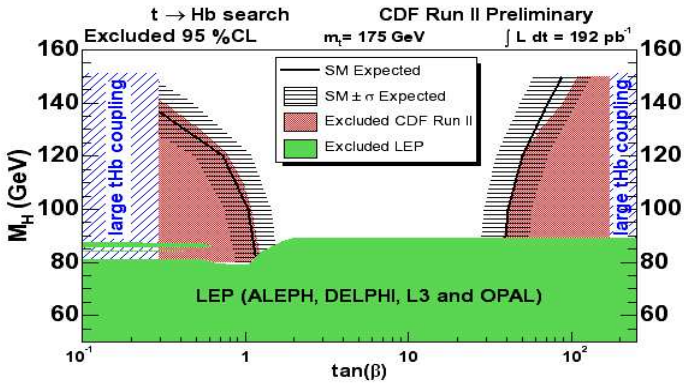

Figure 13: *CDF charged Higgs search. Charged Higgs limits in the $m_{H^\pm}$ vs. $\tan\beta$ plane. The pink regions have been excluded, and the black lines with error bars indicate the expected limit.*

$\ell + \tau$ events [30] to place limits on $t \to H^+ b$ decays in the $m_{H^\pm}$ vs. $\tan\beta$ plane, as shown in figure 13.

Both CDF and DØ have compared their $t\bar{t}$ cross-section measurements obtained with different numbers of b tagged jets to determine the branching ratio $Br(t \to Wb)/Br(t \to Wq)$, where q denotes any down-type quark. The results are [31]

$$\begin{array}{ll} 1.11^{+0.21}_{-0.19} & \text{CDF, } 162\,\text{pb}^{-1}, \\ 0.65^{+0.34}_{-0.30}(\text{stat.})^{+0.17}_{-0.12}(\text{syst.}) & \text{DØ, } 158-169\,\text{pb}^{-1}, \text{ and} \\ 0.70^{+0.27}_{-0.24}(\text{stat.})^{+0.11}_{-0.10}(\text{syst.}) & \text{DØ, } 158-169\,\text{pb}^{-1}, \end{array} \tag{23}$$

where the first DØ result has been obtained with impact parameter b tagging and the second with secondary vertex b tagging. They show no sign of a deviation from the Standard Model expectation close to 1. It should be noted that this quantity does not constrain the value of $|V_{tb}|^2$ in models where top quark decays into quarks from more than three quark generations are allowed.

In summary, from measurements of $t\bar{t}$ production, there is currently no sign of physics beyond the Standard Model.

5 Search for Single Top Quark Production

The production cross-section for single top quarks is proportional to $|V_{tb}|^2$. Also, any differences to the Standard Model prediction could provide hints for new physics.

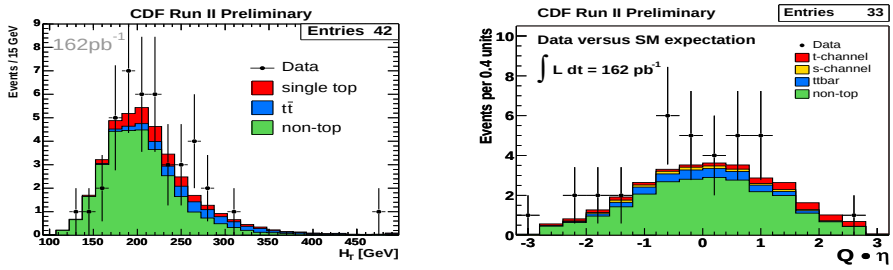

Figure 14: *CDF single top search: The H_T distribution for single top quark candidate events at CDF (left) and the lepton charge signed η distribution of the b jet (right) together with the Standard Model expectations for non-top and $t\bar{t}$ backgrounds and single top signal (the contributions from s-channel and t-channel events are shown separately in the right plot).*

In their searches for single top quark production, the Tevatron experiments concentrate on s-channel and t-channel production with expected cross-sections of 0.9 pb and 2.0 pb, respectively, see figure 1.

Both CDF and DØ select events with an energetic isolated charged lepton, missing transverse energy, and exactly 2 (CDF) or 2–4 (DØ) jets out of which at least one must be b tagged. CDF then selects events with a reconstructed top quark mass between 140 GeV and 210 GeV, while DØ requires $H_T > 150$ GeV. As shown in figure 14, single top events can be found at intermediate values of H_T, and s-channel and t-channel events can be disentangled using the lepton charge signed distribution of the pseudorapidity of the identified b jet. With the current data sets, sensitivity for Standard Model single top quark production has not yet been reached. No significant excess of events has been observed, and the following 95% confidence level limits have been placed on the single top quark cross-section [32]:

experiment	s − channel	t − channel	s+t − channel
CDF	13.6 pb	10.1 pb	17.8 pb
DØ	19 pb	25 pb	23 pb

(24)

With more data being taken and analysed and refined methods being developed, sensitivity for Standard Model single top quark production is within reach for Tevatron Run II.

6 Conclusions

The current status of top quark measurements at the Tevatron experiments CDF and DØ has been summarized, with the exception of the results for the

top quark mass which are covered in a separate article [1].

A wealth of measurements of the total $t\bar{t}$ production cross-section are available from Tevatron Run II. Measurements have been performed for dilepton, lepton+jets, all-hadronic events, and events with top quark decays involving τ leptons. They all yield results that are both mutually consistent and in agreement with the Standard Model prediction.

The event samples have been further interpreted by looking for non-Standard Model $t\bar{t}$ production mechanisms and top quark decays. No signs for physics beyond the Standard Model have been found so far, supporting the interpretation of the signal as $t\bar{t}$ production via QCD and top quark decay to Wb final states.

In the search for single (electroweak) production of top quarks, the sensitivity of the experiments has been improved over Run I. Even for Standard Model single top quark production, a significant cross-section measurement at the Tevatron is within reach in the near future.

7 Acknowledgements

The author would like to thank the organizers for a very interesting and enjoyable conference.

References

1. G. Velev, Top Mass Measurement at Tevatron Run II, these proceedings.
2. N. Kidonakis and R. Vogt, Phys. Rev. **D68**, 114014 (2004),
   N. Kidonakis and R. Vogt, Eur. Phys. J. **C**, S466 (2004).
3. Z. Sullivan, Phys. Ref. **D70**, 114012 (2004).
4. DØ Collaboration, DØ note **4510**.
5. CDF Collaboration, CDF note **7154**. Updated values can be found at http://www-cdf.fnal.gov/physics/new/top/top.html .
6. DØ Collaboration, DØ notes **4422/4423**. Updated values can be found at http://www-d0.fnal.gov/Run2Physics/top/ .
7. DØ Collaboration, DØ note **4625**. Updated values can be found at http://www-d0.fnal.gov/Run2Physics/top/ .
8. DØ Collaboration, DØ note **4206**.
9. CDF Collaboration, Phys. Rev. **D71**, 052003 (2005). Updated values can be found at
   http://www-cdf.fnal.gov/physics/new/top/top.html .

10. CDF Collaboration, Phys. Rev. **D71**, 072003 (2005).

11. CDF Collaboration,
http://www-cdf.fnal.gov/physics/new/top/public/ljets/LooseTagger/ .

12. CDF Collaboration, CDF note **7236**.

13. CDF Collaboration, CDF note **7174**.

14. CDF Collaboration, Phys. Rev. Lett. **93**, 142001 (2004).

15. CDF Collaboration, CDF note **7192**.

16. DØ Collaboration, DØ note **4623**.

17. DØ Collaboration, DØ note **4528**.

18. CDF Collaboration, CDF note **7075**.

19. DØ Collaboration, DØ note **4428**.

20. CDF Collaboration, CDF note **7179**.

21. CDF Collaboration, FERMILAB-PUB-**04-396-E**, hep-ex/0412042.

22. CDF Collaboration, CDF note **7113**.

23. CDF Collaboration, CDF note **7058**.

24. CDF Collaboration, CDF note **7173**.

25. DØ Collaboration, FERMILAB-PUB-**04-057-E**, hep-ex/0404040.

26. DØ Collaboration, DØ note **4549**.

27. DØ Collaboration, DØ note **4545**.

28. CDF Collaboration, Phys. Rev. **D71**, 031101 (2005).

29. M. Beneke *et al*, CERN-TH-**2000-100**, hep-ph/0003033.

30. CDF Collaboration, CDF note **7250**.

31. CDF Collaboration, CDF note **7172**,
DØ Collaboration, DØ note **4586**.

32. CDF Collaboration, Phys. Rev. **D71**, 012005 (2005),
DØ Collaboration, DØ note **4510**.
An updated DØ analysis is available in DØ Collaboration, DØ note **4722**.